A search for light dark matter in XENON10 data

XENON100 Collaboration ; Angle, J ; Baudis, L

Abstract: We report results of a search for light (10 GeV) particle dark matter with the XENON10 detector. The event trigger was sensitive to a single electron, with the analysis threshold of 5 electrons corresponding to 1.4 keV nuclear recoil energy. Considering spin-independent dark matter-nucleon scattering, we exclude cross sections n>7×10-42 cm2, for a dark matter particle mass m =7 GeV. We find that our data strongly constrain recent elastic dark matter interpretations of excess low-energy events observed by CoGeNT and CRESST-II, as well as the DAMA annual modulation signal. © 2011 American Physical Society

DOI: https://doi.org/10.1103/PhysRevLett.107.051301

A search for light dark matter in XENON10 data

J. Angle,[1,2] E. Aprile,[3] F. Arneodo,[4] L. Baudis,[2] A. Bernstein,[5] A.I. Bolozdynya,[6] L.C.C. Coelho,[7] C.E. Dahl,[8] L. DeViveiros,[9] A.D. Ferella,[2,4] L.M.P. Fernandes,[7] S. Fiorucci,[9] R.J. Gaitskell,[9] K.L. Giboni,[3] R. Gomez,[10] R. Hasty,[11] L. Kastens,[11] J. Kwong,[8] J.A.M. Lopes,[7] N. Madden,[5] A. Manalaysay,[1,2] A. Manzur,[11] D.N. McKinsey,[11] M.E. Monzani,[3] K. Ni,[11] U. Oberlack,[10,12] J. Orboeck,[13] G. Plante,[3] R. Santorelli,[3] J.M.F. dos Santos,[7] S. Schulte,[13] P. Shagin,[10] T. Shutt,[6] P. Sorensen,[5,*] C. Winant,[5] and M. Yamashita[3]

(XENON10 Collaboration)

[1] *Department of Physics, University of Florida, Gainesville, FL 32611, USA*
[2] *Physics Institute, University of Zürich, Winterthurerstrasse 190, CH-8057, Zürich, Switzerland*
[3] *Department of Physics, Columbia University, New York, NY 10027, USA*
[4] *Gran Sasso National Laboratory, Assergi, L'Aquila, 67010, Italy*
[5] *Lawrence Livermore National Laboratory, 7000 East Ave., Livermore, CA 94550, USA*
[6] *Department of Physics, Case Western Reserve University, Cleveland, OH 44106, USA*
[7] *Department of Physics, University of Coimbra, R. Larga, 3004-516, Coimbra, Portugal*
[8] *Department of Physics, Princeton University, Princeton, NJ 08540, USA*
[9] *Department of Physics, Brown University, Providence, RI 02912, USA*
[10] *Department of Physics and Astronomy, Rice University, Houston, TX 77251, USA*
[11] *Department of Physics, Yale University, New Haven, CT 06511, USA*
[12] *Johannes Gutenberg University Mainz, 55099 Mainz,Germany*
[13] *Department of Physics, RWTH Aachen University, Aachen, 52074, Germany*

(Dated: August 16, 2011)

We report results of a search for light ($\lesssim$ 10 GeV) particle dark matter with the XENON10 detector. The event trigger was sensitive to a single electron, with the analysis threshold of 5 electrons corresponding to 1.4 keV nuclear recoil energy. Considering spin-independent dark matter-nucleon scattering, we exclude cross sections $\sigma_n > 3.5 \times 10^{-42}$ cm^2, for a dark matter particle mass $m_\chi = 8$ GeV. We find that our data strongly constrain recent elastic dark matter interpretations of excess low-energy events observed by CoGeNT and CRESST-II, as well as the DAMA annual modulation signal.

Recently, the CRESST-II and CoGeNT collaborations have reported the observation of low-energy events in excess of known backgrounds [1, 2]. This has encouraged the hypothesis that these signals − in addition to the long-standing DAMA [3] annual modulation signal − might arise from the scattering of a light ($\lesssim$ 10 GeV) dark matter particle [4–10]. The CDMS [11, 12] dark matter search data been have re-analyzed with lowered energy thresholds, but do not fully exclude light dark matter interpretations. In order to maintain sensitivity to the scattering of such light galactic dark matter, an experiment needs either a very low $\mathcal{O}$(keV) energy threshold, as with CoGeNT, or light target nuclei, such as the oxygen atoms in the CRESST-II detector. This is a simple requirement of the kinematics [13]. For example, consider a halo-bound dark matter particle with mass $m_\chi = 10$ GeV and velocity 600 km s^{-1}. The maximum recoil energy that would result from an elastic scatter of such a particle in an earth-bound target would be about 20 keV for a recoiling oxygen nucleus (CRESST-II), 9 keV for germanium (CoGeNT) and only 6 keV for xenon. The respective energy thresholds of CRESST-II and CoGeNT are approximately 10 keV [14] and < 1 keV [2], which combined with a low background event rate results in good sensitivity to light mass dark matter. The energy threshold of previously reported XENON10 data [15–17] depended on the primary scintillation efficiency of liquid xenon for nuclear recoils ($\mathcal{L}_{eff}$) [18, 19]. For a conservative assumption of the energy dependence of $\mathcal{L}_{eff}$ [18], the threshold was about 5 keV.

It is possible to obtain a lower energy threshold from existing XENON10 dark matter search data, if nuclear recoil energy is measured by the detected electron signal. The method allows us to reach an energy threshold $E_{nr} \sim 1$ keV. At such low nuclear recoil energies, the primary scintillation signal is generally absent. As a result, two important aspects of the XENON10 detector performance are compromised: the ability to precisely reconstruct the z coordinate of a particle interaction, and the discrimination between incident particle types. The detected ratio of scintillation to electron signals was used in [15–17] to discriminate and reject about 99.5% of background events which would otherwise have been treated as dark matter candidate events. Loss of this discrimination thus reduces our sensitivity to nuclear recoils from dark matter particles by about two orders of magnitude. Still, the lower energy threshold we obtain permits the exploration of new regions of dark matter particle mass (m_χ) and cross section (σ_n) parameter space.

The XENON10 detector [15–17, 20] is a liquid xenon time-projection chamber with an active target mass of 13.7 kg (15 cm height and 10 cm radius). It operated dur-

ing 2006-2007 at the Laboratori Nazionali del Gran Sasso in Italy. It was designed to directly detect galactic dark matter particles which scatter off xenon nuclei. Typical velocities of halo-bound dark matter particles are of order 10^{-3}c. This leads to the prediction of a featureless exponential recoil energy spectrum for spin-independent elastic scattering of dark matter particles on a xenon target [21], with typical deposited nuclear recoil energies of a few to tens of keV. A particle interaction in liquid xenon creates both excited and ionized atoms [22, 23], which react with the surrounding xenon atoms to form excimers. The excimers relax on a time scale of 10^{-8} s with the release of scintillation photons. In XENON10, this prompt scintillation light is detected by 88 photomultiplier tubes (47 above the active target, and 41 below) and is referred to as the S1 signal. An electric field $E_d = 0.73$ kV cm^{-1} across the active liquid xenon target causes a large fraction of electron-ion pairs to be drifted away from an interaction site. The electrons are extracted from the liquid xenon and accelerated through a few mm of xenon gas by a stronger electric field $\gtrsim$ 10 kV cm^{-1}, creating a secondary scintillation signal. This scintillation light is detected by the same photo-multiplier tubes, is proportional to the number of electrons and is referred to as S2. The XENON10 detector measures 24 ± 1 photoelectrons per electron extracted from the liquid target. It is this robust signal that gives the S2 channel its lower energy threshold.

The (x, y) coordinates of a particle interaction are reconstructed from the hit pattern of the S2 signal on the top 47 photomultipliers [24]. A cloud of electrons resulting from a particle interaction drifts through the liquid xenon target at $v_d \simeq 0.20$ cm μs^{-1} [25], as a result of E_d. The z coordinate is reconstructed from $z = v_d \Delta t$, where Δt is the measured time delay between the S1 and S2 signals. This method cannot be used if there is no S1 signal, as is often the case for very low energy nuclear recoils [26]. However, the spatial extent of the electron cloud broadens as it drifts, due to diffusion. The longitudinal diffusion D_L [23] is reflected in the width σ_e of the S2 pulse, given by $\sigma_e = (2D_L\Delta t/v_d^2 + \sigma_0^2)^{1/2}$, with the electric field-dependent $D_L = 12$ cm^2 s^{-1} [27]. The constant $\sigma_0 = 0.19$ μs. An approximate z coordinate can therefore be inferred for each scatter vertex, based on σ_e. Although the precision is poorer than can be achieved for events with known Δt, a preferential rejection of edge (in z) events can be achieved. This lowers the background event rate in our central fiducial target. The acceptance as a function of z is shown in Fig. 1.

Ideally we would like to reconstruct the nuclear recoil energy for each event from $\mathrm{E}_{nr} = \epsilon(n_\gamma + n_e)/f_n$, as in [28, 29], with $\epsilon = 13.8$ eV the average energy to create a photon or electron, and f_n the nuclear recoil quenching [30]. However, at low recoil energies the small number n_γ of primary scintillation photons often does not result in a measurable S1 response. Since we are interested in events

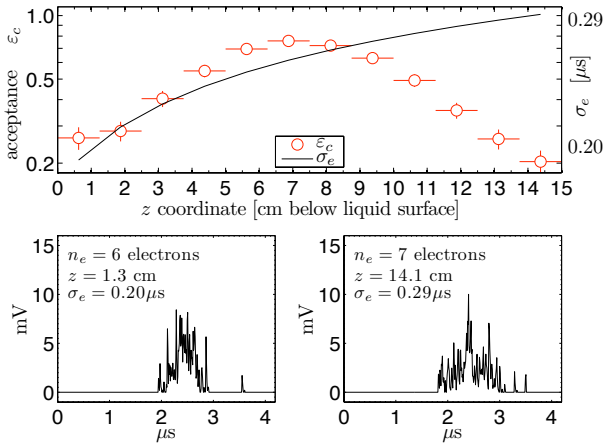

FIG. 1. **(top panel)** Mean S2 pulse width σ_e (curve, right scale), and event acceptance if we require $0.22 < \sigma_e < 0.28$ μs (○, left scale), obtained from single scatter neutron-induced nuclear recoil events with known Δt. Analyses which required an S1 signal [15–17] had full acceptance for $2.8 < z < 12.2$ cm, and no acceptance outside this region. **(bottom panels)** The S2 signal for typical low-energy single scatter nuclear recoils.

at very low recoil energy, we calibrate the energy scale using only the number n_e of measured electrons in the S2 signal. The electron yield of liquid xenon for nuclear recoils has been measured directly using tagged neutron scattering [18, 31]. The lowest-energy data point from [18] implies an S2 signal of 36 ± 6 electrons in the $3-5$ keV range, as shown in Fig. 2. An indirect measurement of the electron yield is described in [32], and was obtained following the method detailed in [26]. The central and $\pm1\sigma$ contours of that work are shown in Fig. 2 (dash-dot curves). That $\mathcal{Q}_y$ rises with decreasing E_{nr} between 100 and 10 keV is a result of the increasing fraction of nuclear recoil energy given to electrons (rather than photons) over that energy range [28].

Following [28], we obtain a theoretical prediction for the electron yield,

$$\mathcal{Q}_y \equiv \frac{n_e}{\mathrm{E}_{nr}} = \frac{1}{\xi}\ln(1+\xi)\frac{f_n(k)/\epsilon}{1+N_{ex}/N_i}. \qquad (1)$$

In this equation, N_{ex}/N_i is the number ratio of excited to ionized xenon atoms, and $\xi = N_i\alpha/(4a^2v)$ is the single parameter upon which the Thomas-Imel box model depends [33, 34]. In Eq. 1 we explicitly indicate the dependence of f_n on the proportionality constant k, between the velocity of a xenon nucleus and its electronic stopping power. In Fig. 2 we show Eq. 1 predictions for two k values, which correspond to calculations by Lindhard [30] and Hitachi [31]. The dashed curve is the best-fit case from [28], with $k = 0.166$, $N_{ex}/N_i = 1.05$ and $\alpha/(a^2v) = 0.024$. The solid curve, which we will use in the present work, takes the more conservative $k = 0.110$, from which we obtain the best-fit parameters $N_{ex}/N_i = 1.09$ and $\alpha/(a^2v) = 0.032$. This results

in the most conservative exclusion limits based on available data and theoretical considerations, and is consistent with our neutron calibration data [32]. However, it is in tension with the measurements of Ref. [18] below ~ 7 keV. As discussed in [35], the rising measured $\mathcal{Q}_y$ values in this regime could be influenced by trigger threshold bias.

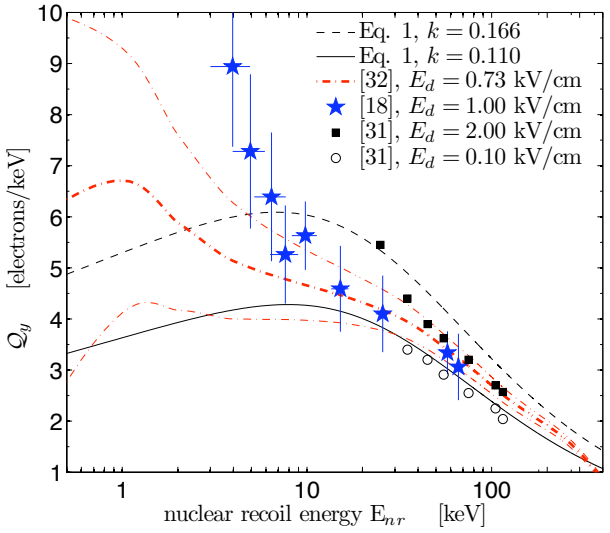

FIG. 2. The electron yield $\mathcal{Q}_y$ of liquid xenon for nuclear recoils. Theoretical curves (solid and dashed) were calculated following [28], as described in the text. Also showing measurements from [18] (★), [31] (○ and ■, uncertainty omitted for clarity), and [32] (dash-dot curve, with $\pm 1\sigma$ contours).

We report results from a 12.5 live day exposure of the XENON10 detector, obtained between August 23 and September 14, 2006. This data set is distinct from the previously reported [15–17] dark matter search data. The difference is that the present data was obtained with the S2-sensitive trigger threshold set at the level of a single electron.

Event selection criteria, which are summarized in Table I, were applied as follows. A radial position $r < 3$ cm was required. This central region features optimal self-shielding by the surrounding xenon target. Discrimination of events with excessive single electron S2 noise was obtained with a signal-to-noise cut, that required the primary pulse to represent at least 0.45 of the total area of the event record. The energy dependence of this cut rises monotonically from 0.94 to > 0.99 between 1.4 keV and 10 keV. Valid single scatter events were required to have only a single S2 pulse of size > 4 electrons. Events in which an S1 signal was found were required to have $\log_{10}(\mathrm{S2/S1})$ within the $\pm 3\sigma$ band for elastic single scatter nuclear recoils. This band was determined from the neutron calibration data, and has been reported in a previous article [15]. Events in which no S1 signal was found were assumed to be low-energy nuclear recoil candidates and were retained.

TABLE I. Summary of cuts applied to 15 kg-days of dark matter search data, corresponding acceptance for nuclear recoils ε_c and number of events remaining in the range $1.4 < \mathrm{E}_{nr} \leq 10$ keV.

Cut description	ε_c	N_{evts}
1. event localization $r < 3$ cm	1.00^a	125
2. signal-to-noise	> 0.94	57
3. single scatter (single S2)	> 0.99	37
4. $\pm 3\sigma$ nuclear recoil band	> 0.99	22
5. edge (in z) event rejection	0.41^b	7

[a] limits effective target mass to 1.2 kg

[b] differential acceptance shown in Fig. 1

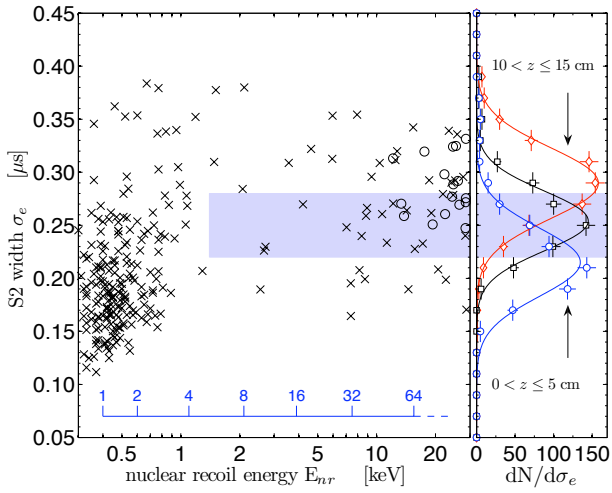

FIG. 3. **(left panel)** All candidate dark matter events remaining (× and ○) after the first four cuts listed in Table I. The fifth cut is indicated by the shaded region. Events in which an S1 was found are shown as ○. The corresponding number of electrons in the S2 signal is indicated by the inset scale. **(right panel)** S2 pulse width distributions for single scatter nuclear recoils in the top, middle and bottom third of the detector.

The remaining events in the lowest-energy region are shown in Fig. 3 versus their S2 pulse width σ_e. The equivalent number of electrons is indicated by the inset scale. A large background population of single electron events is observed. The exact origin of this population is uncertain, although it has been conjectured to arise from photon scattering on impurities in the xenon [36]. Events in which an S1 signal was observed are indicated by a circle.

We use σ_e to discriminate events in the center of the active target from those near the top or bottom. The right panel of Fig. 3 shows the width profiles of nuclear recoils with known Δt for three populations, defined on the intervals $0 < z \leq 5$ cm, $5 < z \leq 10$ cm and $10 < z \leq 15$ cm. Gaussian fits are shown to guide the eye.

The shaded region defining $0.22 < \sigma_e < 0.28$ μs (Table I, line 5) corresponds to $\mu \pm \sigma$ for the central $5 < z \leq 10$ cm population. The fraction of accepted events versus z coordinate for this region is shown in Fig. 1. Based on nuclear recoil events with known Δt, the acceptance of the σ_e cut is a flat $\varepsilon_c = 0.41 \pm 0.01$ in the range $1.4 < \mathrm{E}_{nr} \leq 10$ keV.

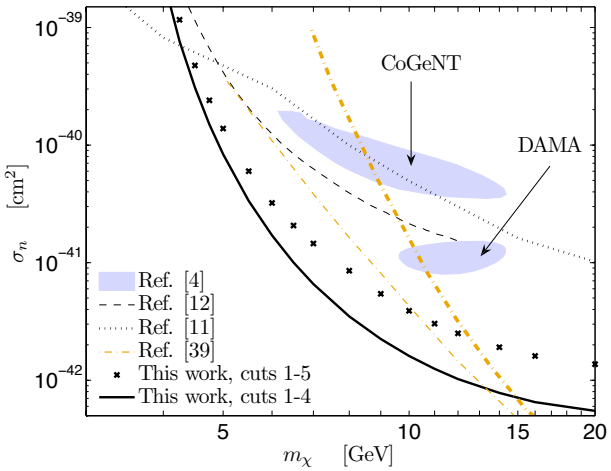

FIG. 4. Curves indicate 90% C.L. exclusion limits on spin-independent σ_n for elastic dark matter scattering, obtained by CDMS (dotted [11] and dashed [12]), XENON100 (dash-dot [39]). 99% C.L. allowed regions consistent with the assumption of a positive detection are also shown, for signals from DAMA (with ion channeling) [4], and CoGeNT (assuming 30% exponential background) [4].

The energy resolution for S2 signals depends primarily on Poisson fluctuation in the number of detected electrons, with an additional component due to instrumental fluctuations. This is discussed in detail in [35], and for higher energy signals in [20]. So as not to overstate the energy resolution, we adopt a parameterization which follows the Poisson component only, given by $\mathcal{R}(\mathrm{E}_{nr}) = (2\mathrm{E}_{nr})^{-1/2}$. We assume a sharp cutoff in $\mathcal{Q}_y$ at $\mathrm{E}_{nr} = 1.4$ keV, and then convolve the resolution with the predicted differential dark matter scattering rate. This procedure ensures that exclusion limits are not influenced by lower-energy extrapolation of the detector response. The scattering rate as a function of nuclear recoil energy was calculated in the usual manner [13] (*cf.* [15]). We take the rotational speed of the local standard of rest and the velocity dispersion of the dark matter halo to be $v_0 = 230$ km s^{-1}, and the galactic escape velocity to be $v_{esc} = 600$ km s^{-1} [37].

We use the p_{max} method [38] to calculate 90% CL exclusion limits on allowed regions of elastic spin-independent dark matter parameter space in the $\sigma_n - m_\chi$ plane, treating all remaining events in the the range $\mathrm{E}_{nr} > 1.4$ keV as potential dark matter signal. This lower bound is indicated by the left-most edge of the shaded region in Fig. 3, and corresponds to an S2 signal of 5 electrons. The results are shown in Fig. 4. Surprisingly, the sensitivity is poorer after applying edge (in z) event rejection based on σ_e. This is due to the small electron diffusion coefficient D_L under our operating conditions, and the relatively modest $z = 15$ cm electron drift distance across the xenon target. Larger detectors [39, 40], if operated with a lower value of E_d, should expect to obtain a significant improvement in sensitivity from this technique [27].

The exclusion limits and allowed regions shown in Fig. 4 assume a simple Maxwell-Boltzman distribution for the dark matter halo. Given the likelihood of significant departures from this distribution [41], it is important to understand if astrophysical uncertainties could alter the incompatibility of our results with the positive detection scenarios shown in Fig. 4. A method for doing so is described in [42], and predicts that not less than ~ 5 counts keV^{-1} kg^{-1} day^{-1} (dru) should be observed in a xenon detector, if the unexplained low-energy rise observed by the CoGeNT detector [2] were due to dark matter scattering. It can be seen from Table I that we observe an event rate of ~ 0.2 dru on the interval $1.4 < \mathrm{E}_{nr} < 10$ keV. In other words, the order of magnitude exclusion of the CoGeNT region shown in Fig. 4 is robust against astrophysical uncertainties. Due to the preliminary nature of the CRESST-II results we do not show a corresponding allowed region, although it appears likely to lie above the DAMA region, as shown in Fig. 4 of Ref. [43].

We have shown for the first time that it is possible to perform a sensitive search for dark matter with a liquid xenon time-projection chamber, using only the electron signal. The advantage of this analysis is an increased sensitivity to light ($\lesssim 10$ GeV) dark matter candidate particles, due to the approximate factor $\times 5$ decrease in the detector energy threshold. For larger particle masses, standard analyses [15, 16, 39, 44] offer superior sensitivity. The present work appears to severely constrain recent light elastic dark matter interpretations of the excess low-energy events observed by CoGeNT and CRESST-II, as well as interpretations of the DAMA modulation signal.

This work was initiated at the KITP workshop "Direct, Indirect and Collider Signals of Dark Matter," Santa Barbara CA, December 7-18, 2009, which was supported in part by the National Science Foundation under Grant No. PHY-05-51164. We gratefully acknowledge support from NSF Grants No. PHY-03-02646 and No. PHY-04-00596, CAREER Grant No. PHY-0542066, DOE Grant No. DE-FG02-91ER40688, NIH Grant No. RR19895, SNF Grant No. 20-118119, FCT Grant No. POCI/FIS/60534/2004 and the Volskwagen Foundation.

* pfs@llnl.gov

[1] W. Seidel (CRESST-II) lecture at "Identication of Dark Matter 2010" conference, University of Montpellier 2, Montpellier FR, July 26-30, 2010.

[2] C.E. Aalseth *et al.* (CoGeNT Collaboration), Phys. Rev. Lett. **106** 131301 (2011).

[3] R. Bernabei *et al*, Eur. Phys. J. C **56** 333 (2008).

[4] S. Chang, J. Liu, A. Pierce, N. Weiner and I. Yavin, J. Cosmol. Astropart. Phys. **08** 018 (2010).

[5] P.W. Graham, R. Harnik, S. Rajendran and P. Saraswat, Phys. Rev. D **82** 063512 (2010).

[6] R. Essig, J. Kaplan, P. Schuster and N. Toro, arXiv:1004.0691 (2010).

[7] D. Hooper, J.I. Collar, J. Hall, D.N. McKinsey and C.M. Kelso, Phys. Rev. D **82** 123509 (2010).

[8] A.L. Fitzpatrick and K.M. Zurek, Phys. Rev. D **82**, 075004 (2010).

[9] B. Feldstein, P.W. Graham and S. Rajendran, Phys. Rev. D **82** 075019 (2010).

[10] A. Bottino, F. Donato, N. Fornengo and S. Scopel, Phys. Rev. D **81** 107302 (2010).

[11] D.S. Akerib *et al.* (CDMS Collaboration), Phys. Rev. D **82** 122004 (2010).

[12] Z. Ahmed *et al.* (CDMS Collaboration), arXiv:1011.2482 (2010).

[13] J.D. Lewin and P.F. Smith, Astropart. Phys. **6** 87 (1996).

[14] G. Angloher *et al.*, Astropart. Phys. **31** 270 (2009).

[15] J. Angle *et al.* (XENON10 Collaboration), Phys. Rev. D **80**, 115005 (2009).

[16] J. Angle *et al.* (XENON10 Collaboration), Phys. Rev. Lett. **101** 091301 (2008).

[17] J. Angle *et al.* (XENON10 Collaboration), Phys. Rev. Lett. **100** 021303 (2008).

[18] A. Manzur *et al.*, Phys. Rev. C **81**, 025808 (2010).

[19] E. Aprile *et al.*, Phys. Rev. C **79**, 045807 (2009).

[20] E. Aprile *et al.* (XENON10 Collaboration), Astropart. Phys. **34** 679 (2010).

[21] G. Jungman, M. Kamionkowski and K. Griest, Phys. Rept. **267** (1996).

[22] S. Kubota *et al.*, Phys. Rev. B **17** 2762 (1978).

[23] E. Aprile and T. Doke, Rev. Mod. Phys. **82** 2053 (2010).

[24] J. Angle *et al.* (XENON10 Collaboration), Nucl. Phys. B Proc. Suppl. **173** 117 (2007).

[25] E.M. Gushchin, A.A. Kruglov and I.M. Obodovskii, Sov. Phys. JETP **55** 650 (1982).

[26] P. Sorensen *et al.* (XENON10 Collaboration), Nucl. Instr. Meth. A **601**, 339 (2009).

[27] P. Sorensen, Nucl. Instr. Meth. A **635** 41 (2011).

[28] P. Sorensen and C.E. Dahl, Phys. Rev. D **83** 063501 (2011).

[29] T. Shutt *et al.*, Nucl. Instr. Meth. A **579** 451 (2007).

[30] J. Lindhard, V Nielsen, M. Scharff and P.V. Thomsen, Mat. Fys. Medd. Dan. Vid. Selsk. **33** 10 (1963).

[31] E. Aprile *et al.*, Phys. Rev. Lett. **97** 081302 (2006).

[32] P. Sorensen *et al.* (XENON10 Collaboration), PoS (IDM2010)017 (2010), arXiv:1011.6439.

[33] J. Thomas and D.A. Imel, Phys. Rev. A **36** 614 (1987).

[34] The model describes N_i initial electron-ion pairs in a box of dimension a, with recombination coefficient α and average electron drift velocity v.

[35] P. Sorensen, J. Cosmol. Astropart. Phys. **09** 033 (2010).

[36] B. Edwards *et al.* (ZEPLIN-II Collaboration), Astropart. Phys. **30** 54 (2007).

[37] M.C. Smith *et al.*, Mon. Not. Roy. Astron. Soc. **379** (2007) 755772.

[38] S. Yellin, Phys. Rev. D **66**, 032005 (2002).

[39] E. Aprile *et al.* (XENON100 Collaboration), Phys. Rev. Lett. **105** 131302 (2010).

[40] D.N. McKinsey *et al.* (LUX Collaboration), J. Phys.: Conf. Ser. **203** (2010) 012026.

[41] M. Kuhlen *et al.*, J. Cosmol. Astropart. Phys. **02** 030 (2010).

[42] P.J. Fox, J. Liu and N.Weiner, arXiv:1011.1915 (2010).

[43] T. Schwetz, arXiv:1011.5432 (2010).

[44] E. Aprile *et al.* (XENON100 Collaboration), arXiv:1104.2549 (2011).